Evaporative Cooling of Air in Impinging Streams

B. Yao, Y. Berman, and A. Tamir
Dept. of Chemical Engineering, Ben-Gurion University of the Negev, Beer-Sheva 84105, Israel

An experimental study was conducted on evaporative cooling of air in an impinging-stream reactor, in which two droplet gas streams flow in opposite directions and meet in the impingement zone. The air was cooled by evaporation of water droplets. Volumetric heat-transfer coefficients h_v determined enabled us to evaluate the performance of the cooler. Maximum values of h_v varied from 4 to 14 kW/m^3·K. The effectiveness of impinging streams was evaluated by placing a partition in the impingement zone, which prevented interaction between the streams. A numerical modeling of the droplets' behavior in an impinging-stream reactor was also performed on the basis of heat and momentum equations. Effects of initial droplets' size and velocity as well as atomization and coalescence on the enhancement by impinging streams have been investigated. Correlation equations are also discussed. These experimental and numerical results helped understand the fundamental mechanisms of an impinging-stream reactor with a gas-droplet suspension and further verify the effectiveness of the method of impinging streams.

Introduction

Cooling of water is usually conducted by exposing its surface to air so that a small portion of it evaporates and causes the temperature to decrease. This is called evaporative cooling. Cooling of gases is traditionally achieved by their compression and expansion. In this article, an application of evaporative cooling in an impinging-stream reactor for cooling of air is presented, which proved promising. Impinging streams, used as a method for enhancing heat and mass transfer processes, have been studied by Elperin (1972) and further developed by Tamir (1994). The method has been successfully applied for the combustion of gas and coal (Luzzatto and Tamir, 1988; Ziv et al., 1988); drying of solids (Tamir et al., 1984; Tamir and Elperin, 1987; Kitron et al., 1987; Bar and Tamir, 1990); solid-solid and gas-gas mixing (Tamir and Luzzatto, 1985a,b); absorption and desorption of gases from liquids in the presence and in the absence of a chemical reaction (Tamir and Herskowits, 1985; Tamir, 1986; Tamir and Elperin, 1987; Herskowits et al., 1987, 1988); enrichment of phosphate ores (Ziv and Tamir, 1993), preparation of emulsions (Tamir and Sobhi, 1985); liquid-liquid extraction (Herbet, in progress); and dissolution of solids in water (Tamir and Glitzenstein, 1994).

In the impinging-stream reactor in Figure 1, coaxial axisymmetric jets flow in opposite directions and impinge at the stagnation plane. The behavior of gas impinging streams was considered in some investigations (Elperin, 1972; Kostiuk and Libby, 1993; Kostiuk et al., 1993; Champion and Libby, 1993; Tamir, 1994). It has been established that for the calculation of droplet motion, the velocity of the gas in the jets can be assumed constant, and it is equal to zero at the impingement plane, with changing direction of the flow. At the zone of impingement, droplets penetrate into the opposite stream due to their inertia and decelerate until stagnation due to the gas drag force. Afterwards, the droplets accelerate and penetrate into the original stream, and so forth. Thus, droplets perform damped oscillations resulting in the following: (1) the resi-

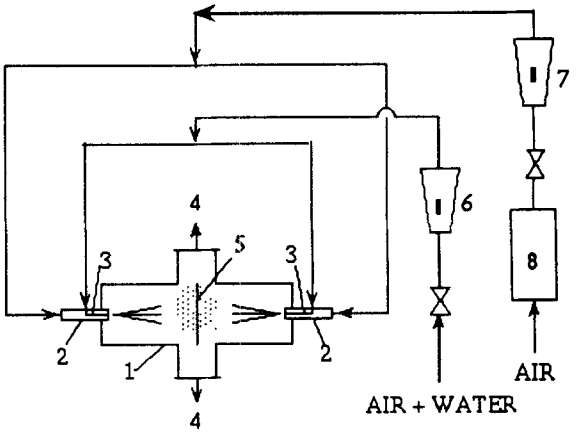

Figure 1. Two impinging-stream evaporative cooler.

Correspondence concerning this article should be addressed to A. Tamir.

dence time of droplets in reactor is increased; (2) the relative velocity between the droplets and the gas phase in the zone of impingement is significantly increased and may reach twice the velocity of the air stream. Thus, the increase of the relative velocity decreases the resistance to the heat and mass transfer in processes where the external resistance predominates. (3) Atomization of the original droplets due to collisions increases the surface area. On the other hand, under some circumstances it is possible to obtain coalescence between droplets that decrease the surface area. In addition, the intensity of turbulence in the stagnation plane, which has a different production mechanism compared with that in the widely studied turbulent shear flows, can be observed (Kostiuk and Libby, 1993). All of these result in the enhancement of the convective heat- and mass-transfer rates between water droplets and the cooled air by comparison to other methods that do not employ impinging streams.

Recently, Kondratov et al. (1989) published a note on evaporative cooling of air by impinging streams, probably the first to do so. The essence of the method lies in exposing air to a fine spray of water where their evaporation causes the air to cool. The experimental system and its operation are similar to that shown in Figure 1. The size of the evaporation chamber of Kondratov et al. was $0.09\times0.07\times0.07$ m, the diameter of the acceleration pipes was 0.03 m, the distance between their faces was 0.04 m where the spray nozzles were with diameter of 0.006 m, and at a distance of 0.41 m from the center of the chamber. It is noted that the amount of the experimental data is small. However, the results indicate the practical potential of evaporative cooling by impinging streams.

The major objectives of the present study (Yao, 1994) were: (1) to measure reliable data of volumetric heat-transfer coefficients, which enables one to evaluate impinging streams by comparison to other methods; (2) to verify the effectiveness of impinging streams for evaporative cooling, which is achieved by placing a partition between the impinging streams, thereby eliminating interaction between the streams and characteristic behaviors; and (3) to model an impinging-stream evaporative cooling process from conservation of momentum and heat equations and correlate the data vs. operation parameters.

Experimental Apparatus and Procedure

Figure 1 consists of the following parts: (1) a cylindrical cooling cell made of Perspex with dimensions of $D(\text{m})\cdot L(\text{m}) = 0.06\times0.084$, 0.06×0.115, 0.06×0.195, 0.138×0.200; (2) inlet pipes with diameters of 0.015 m and lengths of 0.22 m; (3) spray nozzles that atomize water by air pressure; (4) air exits; (5) partition; (6) and (7) rotameters; and (8) air heater. A typical run was conducted as follows. The test is initiated by adjusting powerstats to obtain the desired temperature and setting the time needed to reach a steady-state temperature, which depends on the air velocity. A steady-state temperature of about 60°C is usually obtained within 3 to 4 h. The inlet temperature of air into the cooler and its flow rate were fixed at a prescribed value. The water flow rate was adjusted to a maximum value, ensuring complete evaporation of the spray droplets. These conditions were observed when at the exit of the cooler a minimal amount of droplets could be detected on the palm. From the dry- and wet-bulb temperatures at the inlet and exit of the cooler it was possible to determine the vaporization rate of water and the volumetric heat-transfer coefficient h_v defined by

$$h_v = \frac{q}{V_r \Delta T_{lm}} = \frac{W_a(H_o - H_i)\lambda}{V_r \Delta T_{lm}} \tag{1}$$

where ΔT_{lm} is given by

$$\Delta T_{lm} = \frac{\Delta T_i - \Delta T_o}{\ln \dfrac{\Delta T_i}{\Delta T_o}} \tag{2}$$

where $\Delta T_i = T_i - T_1$, $\Delta T_o = T_o - T_{wb}$, and H_o and H_i are the humidities of inlet and outlet gas, respectively, which are determined by measuring dry- and wet-bulb temperatures. It should be noted that a small error in the humidity value may cause a large error in the results of the heat-transfer coefficient. In order to increase the accuracy, the saturated humidity was correlated vs. temperature by an equation, rather than reading it from the charts.

Results and Discussion

The following parameters were tested in the experiments: air flow rate and its inlet and outlet temperatures, dimensions of the cooler, and the effect of the partition on the heat-transfer coefficients. The range of the operating conditions and the major results without a partition were:

- Air inlet temperature to cooler: 50 to 70°C
- Air exit temperature from cooler: 45 to 65°C
- Temperature drop of air between inlet and exit to cooler: 3.5 to 10°C
- Water temperature: 21.1 to 28.6°C
- Wet-bulb temperature at inlet and exit: 19.8 to 25.8°C
- Absolute pressure in the cooler: about 740 mm Hg
- Pressure drop on cooler: 2 to 40 mm H_2O
- Total air flow rate to cooler: 3×10^{-3} to 14×10^{-3} m^3/s
- Air velocity at inlet pipe to cooler: 9 to 40 m/s
- Water vaporization rate: 7×10^{-6} to 40×10^{-6} kg/s
- Water consumption: 2×10^{-3} to 2.5×10^{-3} kg water/kg air
- Air humidity at inlet to cooler: 0.5×10^{-3} to 5.5×10^{-3} kg water/kg air
- Air humidity at exit from cooler: 1.5×10^{-3} to 7.0×10^{-3} kg water/kg air
- Volumetric heat-transfer coefficient: 450 to 14,0000 $W/m^3\cdot K$
- Power input to transfer the air through the cooler ($Q_g \Delta P$): 0.15 to 5.5 J/s
- Power input: 0.02 to 0.35 kJ/kg air
- Power input: 14 to 190 kJ/kg water
- Power input: 0.45 to 20 kW/m^3 reactor
- Relative distance between accelerating ducts: $5.5 \le L/d \le 13.3$

Effect of air flow rate

Figure 2 demonstrates the dependence of h_v on air velocity at inlet pipes. Since the results correspond to the smallest reactor, the values of h_v are the maximum ones. An increase in h_v by increasing the air flow rate is clearly observed de-

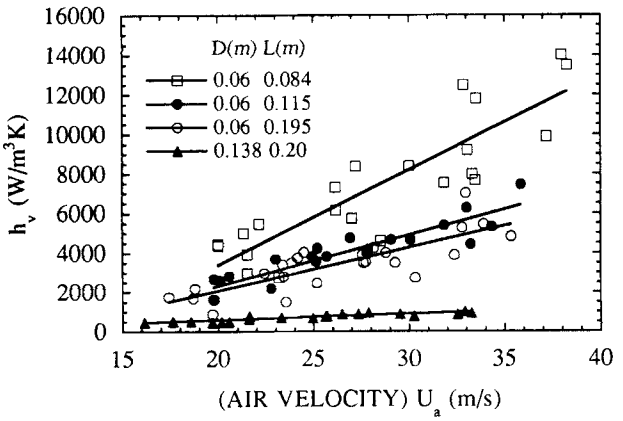

Figure 2. Effect of air velocity on the volumetric heat-transfer coefficients.

spite the scatter of the data caused by the accuracy of the determination of the difference in the humidities of the air between the inlet and the exit of the cooler. This behavior is caused by the reduction of the external resistance to the heat and mass transfer, which controls the evaporative cooling process. The data were correlated by the following expression:

$$h_v(\mathrm{W/m^3 \cdot K}) = AU_a^{\alpha}(\mathrm{m/s}) \tag{3}$$

where A and α are given in Table 1.

It is interesting to note that the exponent α is identical for coolers of an identical diameter D. The diameter determines the air velocity inside the cooler, which is also responsible for the magnitude of α. On the other hand, α for the larger reactor is smaller because the diameter is larger and consequently the velocity in the cooler is smaller for identical flow rates. It is also interesting to note that for coolers of different dimensions and the same D, the rate of evaporation per unit logarithmic temperature difference remains constant within $\pm 20\%$, that is, in Eq. 3 $A \cdot V_r$ = constant, where A is the constant in Table 1. This indicates that the evaporation of water droplets takes place in the jets' volume and is independent of the reactor's dimensions. The latter has also been established in other processes (Tamir, 1994).

Effect of the partition

An accepted method for estimation of the heat-transfer efficiency in impinging streams employs the introduction of a partition midway in the streams. Thus, the particles or droplets perform only the trajectory 1′–2′ in Figure 3c instead of the trajectory 1–2–3–4. Thus, the penetration of

Table 1. Parameters in Eq. 3

Cooler Size D(m)× L(m)	A	α	U_a(m/s)	r*
0.06 ×0.084	14.17	1.85	15–40	0.86
0.06 ×0.115	8.87	1.85	15–40	0.90
0.06 ×0.195	7.58	1.85	15–40	0.79
0.138×0.20	19.35	1.12	15–40	0.91

*r—correlation coefficient.

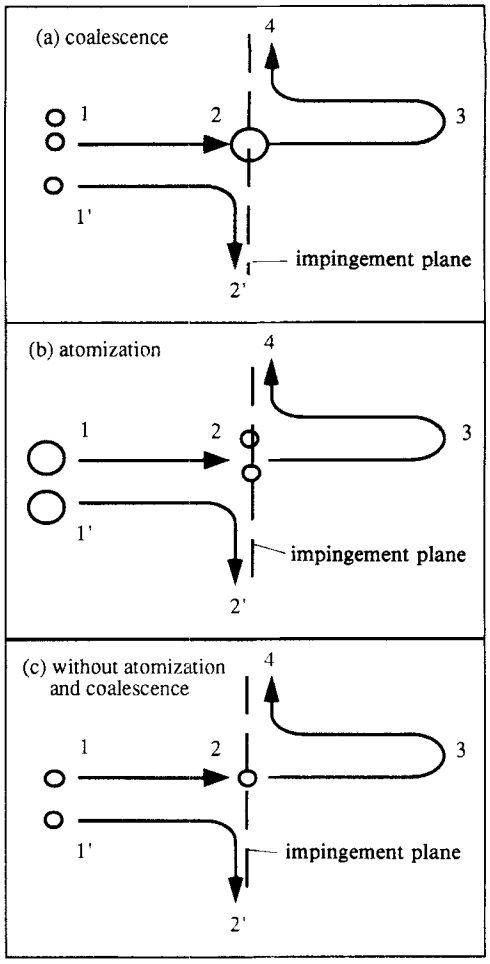

Figure 3. Trajectories of two droplets for evaluation of heat-transfer enhancement.

particles from one stream into the other, which is the key reason for enhancing the heat- and mass-transfer rates in impinging streams, is eliminated, and hence the increase in the heat-transfer rates is reduced. It has been established elsewhere (Tamir, 1994) that the introduction of a partition in various processes (drying, combustion, absorption, calcination of phosphate, etc.) decreased the rate of the process by a factor of 1.5–3.

The effect of impinging streams on the evaporative cooling of air was investigated by placing a partition in the middle of the device, designated as 5 in Figure 1. This partition separated the cooler into two noninteracting compartments. Thus, the following ratio was defined in order to evaluate the enhancement effect of impinging streams:

$$E_h = \frac{\text{rate of heat removal from air without partition}}{\text{rate of heat removal from air with partition}} = \frac{\text{total amount evaporated from droplets without a partition}}{\text{total amount evaporated with a partition}}. \tag{4}$$

Figure 4 demonstrates the effect of the partition as well as the diameter of the cooler and the air flow rate on the volu-

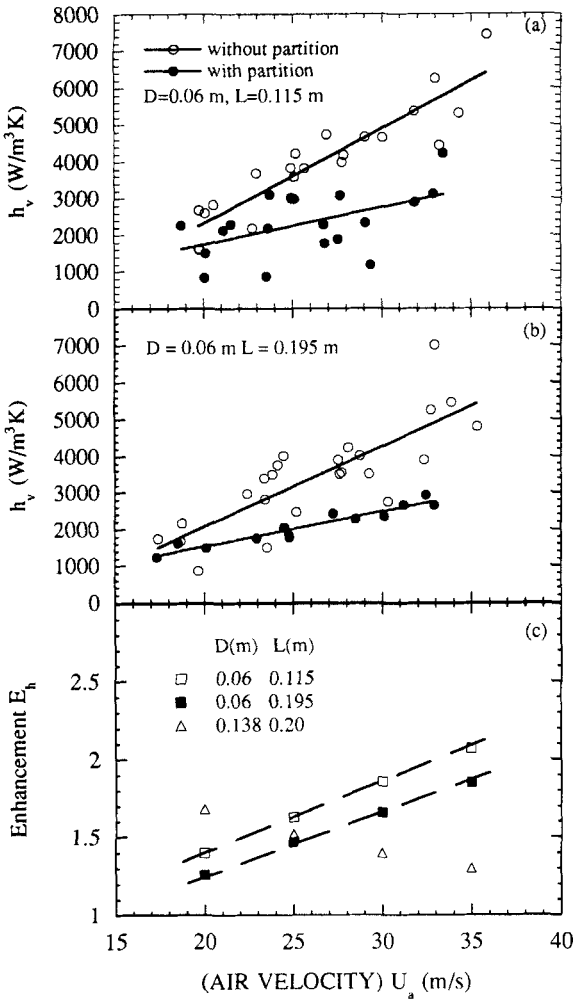

Figure 4. Effect of a partition on evaporative cooling of air.

metric heat-transfer coefficient. The following trends were observed: (1) the partition reduces the heat-transfer coefficient, thus eliminating the enhancement effects of impinging streams; and (2) impinging streams increase the heat removal by a mean value of 50% by comparison to the situation where their effect is absent. This is indicated by the ratio E_h in Figure 4c. As seen, for coolers of $D = 0.06$ m, E_h is increasing vs. the air flow rate. This increase is caused by the increase in the relative velocity between the phases, and hence h_v. However, for $D = 0.138$ m the behavior is opposite because the air velocity is approximately five times lower. Thus, the effect of the relative velocity may not be significant. On the other hand, the mean residence time of the phases in the cooler is appreciably increased, causing higher values of E_h at small air flow rates.

An additional elaboration of the partition's effect is as follows. The partition is hardly affecting the motion of the colliding gas streams. However, the colliding droplets at the end of their trajectory (point 2 in Figure 3c) might create a thin liquid layer on the partition, thus increasing the evaporative cooling of the air in comparison to the case where the partition is absent. The fact that this phenomenon does not occur indicates that the partition has a weakening effect on the heat- and mass-transfer rates.

Modeling

The model visualizes two streams of air moving inside the cooler, one toward the other on the same axis at velocity U_a. Droplets of initial diameter $d_{p,o}$ are introduced into the air streams flowing at an initial velocity U_a and are accelerated toward the impingement plane. The initial velocity of the droplets is $U_{p,o}$. During their motion, the droplets undergo vaporization, causing air cooling. The trajectory of the droplets is 1–2–3–4 in Figure 3 and is composed of the following sections. Along the path 1–2 the droplets accelerate. They decelerate along path 2–3, and accelerate again along 3–4, where at point 4 the droplets are withdrawn from the system. The behavior of the droplets is compared with that of droplets performing the trajectory 1′–2′, where at point 2′ they are removed from the system. Thus, the preceding comparison makes it possible to evaluate the enhancement ratio E_h given by Eq. 4 and to compare it with experimental results. In the following analysis a single droplet is considered for which appropriate equations are available. Additional underlying assumptions are:

- The droplet remains spherical at all times.
- The droplet temperature is uniform throughout and remains constant at its wet-bulb value.
- The sole resistance to the heat transfer from the gas to the droplet is an external one.
- Sensible heat effects are negligible by comparison to the latent heat.

Considering the above assumptions, a heat balance on the droplet yields the following energy equation:

$$\frac{d(d_p)}{dt} = -2\frac{h(T_a - T_{wb})}{\lambda \rho_l} \tag{5}$$

The heat-transfer coefficient between the gas and the droplet is given (Bird et al., 1960) by

$$h = \frac{k'_a}{d_p}\left(2 + 0.552 Re_p^{1/2} Pr^{1/3}\right) \tag{6}$$

where

$$Re_p = \frac{d_p |U_a - U_p|}{\nu_a}; \qquad Pr = \frac{C_{p,a}\,\mu_a}{k'_a}. \tag{7}$$

The equation of motion for the droplet, which is related to the preceding equation through the velocity of the droplet, is obtained from eqs. (5–5), (5–6), and (5–14) of Tamir (1994) for the Stokes' regime where $Re_p < 0.3$. The following equations were obtained:

$$\frac{dU_p}{dt} = 18\frac{\nu_a \rho_a}{\rho_p d_p^2}(U_a - U_p) \qquad \text{acceleration stage} \tag{8}$$

$$\frac{dU_p}{dt} = -18\frac{\nu_a \rho_a}{\rho_p d_p^2}(U_a + U_p) \qquad \text{deceleration stage.} \tag{9}$$

For the intermediate regime where $0.3 < Re_p < 1000$, the following equations were obtained from Eqs. 5–23, 5–25, and 5–34 of Tamir (1994):

$$\frac{dU_p}{dt} = 9.36\frac{\nu_a^{1/2}\rho_a}{\rho_p d_p^{3/2}}(U_a - U_p)^{3/2} \quad \text{acceleration stage} \quad (10)$$

$$\frac{dU_p}{dt} = -9.36\frac{\nu_a^{1/2}\rho_a}{\rho_p d_p^{3/2}}(U_a + U_p)^{3/2} \text{deceleration stage.} \quad (11)$$

It should be noted that in the theoretical analysis it was sufficient to consider only the flow regimes just given. The energy equation and the equation of motion are coupled equations that were integrated simultaneously by the Runge-Kutta technique to obtain the variation of the evaporation rate and droplet radius vs. time. Thus, according to Eq. 4 E_h is given by

$$E_h = \frac{\left(\alpha d_{p,1}^3 - \beta d_{p,4}^3\right)_{\text{trajectory 1-2-3-4 in Figure 4}}}{\gamma\left(d_{p,1'}^3 - d_{p,2'}^3\right)_{\text{trajectory 1'-2' in Figure 4}}} \quad (12)$$

where $d_{p,1}$ and $d_{p,4}$ are, respectively, the diameter of the droplet at points 1 and 4 along the trajectory 1–2–3–4, $d_{p,1'}$ and $d_{p,2'}$ are the diameter of the droplet at points 1′ and 2′ along the trajectory 1′–2′ in Figure 3. In the absence of atomization or coalescence, $\alpha = \beta = \gamma = 1$. In the presence of atomization, $\alpha = 1$, $\beta = 2$, and $\gamma = 1$, whereas in the presence of coalescence, $\alpha = 2$, $\beta = 1$, and $\gamma = 2$.

The influence of atomization and coalescence is based on a comparison between two droplets in Figure 3. In addition to the preceding assumptions, the following assumptions are made for calculating the processes of atomization and coalescence:

- Atomization of a droplet occurs at the impingement plane 2 in Figure 3b. It is assumed that a spherical droplet disintegrates into two spherical droplets of equal mass.
- Interdroplet coalescence is visualized by assuming that two droplets collide at the impingement plane after accelerating separately along the path 1–2 in Figure 3a. From point 2 they move as a single droplet along a deceleration–acceleration path up to exit point 4.
- Atomization or coalescence change the velocity of the droplet but do not change the original flow direction of the newly formed droplets at the impingement plane.

In the presence of atomization, which yields two droplets at point 2, the radius of new droplet $d'_{p,2}$ in Figure 4b is related to the original one by

$$d'_{p,2} = 2^{-1/3} d_{p,2}. \quad (13)$$

Thus, the increase in Eqs. 4 and 12 gave the following expression:

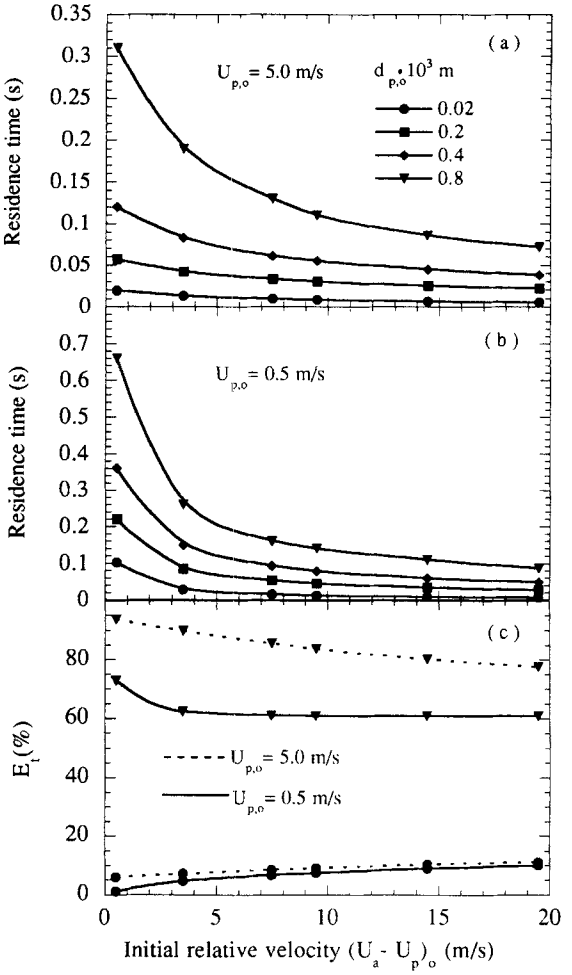

Figure 5. Effect of the initial droplet size $d_{p,o}$ and velocity on its residence time in the cooler.

$$E_h = \frac{\frac{1}{6}\left(d_{p,1}^3 - d_{p,2}^3\right)\lambda\rho + 2\frac{1}{6}\left(d_{p,2}'^3 - d_{p,3}^3\right)\lambda\rho + 2\frac{1}{6}\left(d_{p,3}^3 - d_{p,4}^3\right)\lambda\rho}{\frac{1}{6}\left(d_{p,1}^3 - d_{p,2}^3\right)\lambda\rho}$$

$$= 1 + \frac{\left(d_{p,2}^3 - 2d_{p,4}^3\right)}{\left(d_{p,1}^3 - d_{p,2}^3\right)}. \quad (14)$$

With coalescence, where two droplets form one droplet at point 2 in Figure 3a, the new droplet is related to the original one by

$$d'_{p,2} = 2^{1/3} d_{p,2} \quad (15)$$

$$E_h = 1 + \frac{\left(2d_{p,2}^3 - d_{p,4}^3\right)}{2\left(d_{p,1}^3 - d_{p,2}^3\right)}. \quad (16)$$

The solution of differential equations (Eqs. 8 to 11) is generally a function of the following parameters: initial velocity of the droplet and the relative velocity between the phases;

initial diameter of the droplet: and the temperature of the air as well as the surface temperature of the droplet, which is equal to its wet-bulb temperature. In the calculations, mean experimental values were taken, namely, air temperature T_a = 50°C and water wet-bulb temperature T_{wb} = 20°C.

Effect of the initial droplet size and velocity on its residence time

Figure 5 shows the residence time of the droplet in the cooler, which is an important quantity for explaining the behaviors below, as a function of the initial droplet size $d_{p,o}$, initial relative velocity $(U_a - U_p)_o$ at the inlet of the cooler, and the initial droplet velocity $U_{p,o}$. The general trends observed were (1) residence time decreases by increasing the initial relative velocity $(U_a - U_p)_o$. At small relative velocities, the change in the velocity of the droplet is also small according to Eq. 8; hence, the droplet will stay longer in the system. On the other hand, at large relative velocities, the droplet will accelerate faster, resulting in shorter residence times. (2) The residence time decreases by increasing the initial droplet's velocity $U_{p,o}$. (3) The residence time increases by increasing the initial droplet's diameter, $d_{p,o}$ because large droplets are accelerated more slowly than smaller ones. (4) More insight on these trends can be obtained by considering the ratio E_t by

$$E_t(\%) = \frac{\text{residence time in trajectory 2–3–4 in Figure 3}}{\text{residence time in trajectory 1–2–3–4 in Figure 3}} \tag{17}$$

which is depicted in Figure 5c. It is observed that the biggest droplet moving at a high initial velocity stays most of the time (about 90%) along the first deceleration and second acceleration trajectories in Figure 3c. On the other hand, the smallest droplet stays mainly along the first acceleration path, and the effect of the initial droplet's velocity is negligible.

Effect of the initial droplet size on the enhancement

Figure 6 shows the dependence of the enhancement E_h on the initial droplet's size, relative velocity, and the droplet's velocity. It was found that for large droplets, E_h decreases by increasing the initial relative velocity $(U_a - U_p)_o$, whereas it increases for small droplets. The reason for this behavior is related to the effect of $d_{p,o}$ on the residence time of the droplets demonstrated in Figure 5, where for large droplets the residence time is significantly longer for small values of $(U_a - U_p)_o$ than for larger values of this quantity. Thus, the total amount of heat delivered to the droplet by the air is greater for small values of $(U_a - U_p)_o$.

Effect of the initial droplet velocity on the enhancement

The effect of initial droplet velocity on E_h is shown in Figure 7. It is evident that for a certain value of the droplet's size ($d_{p,o} = 0.02 \times 10^{-3}$ m), the increasing initial droplet velocity would promote the heat-transfer rate between two phases. This occurs because the droplet penetrates further into the opposite stream by air with a higher velocity. Furthermore, the effect of the initial droplet's velocity on E_h is different for different sizes. As the droplet's size increases, an increase in the time it remains becomes more pronounced, as stated before. In addition, large and small droplets show an opposite trend with respect to E_h.

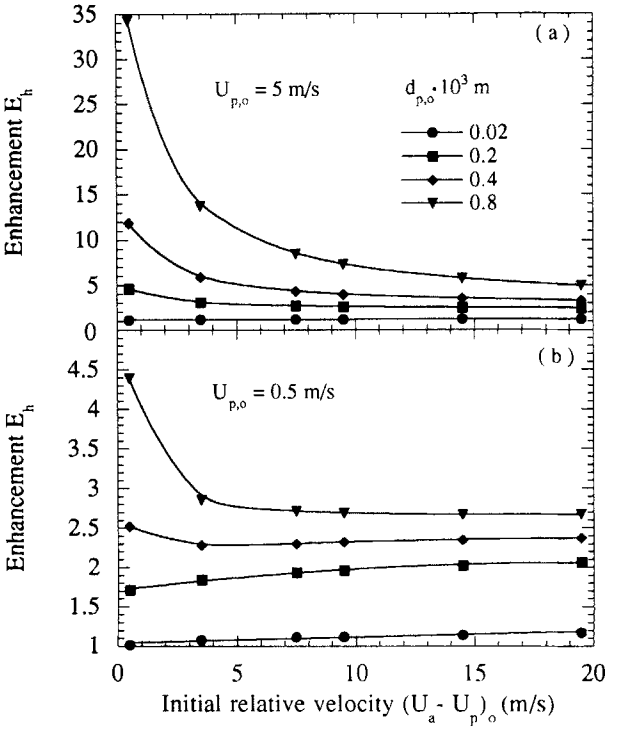

Figure 6. Effect of the initial droplet size $d_{p,o}$ on the enhancement.

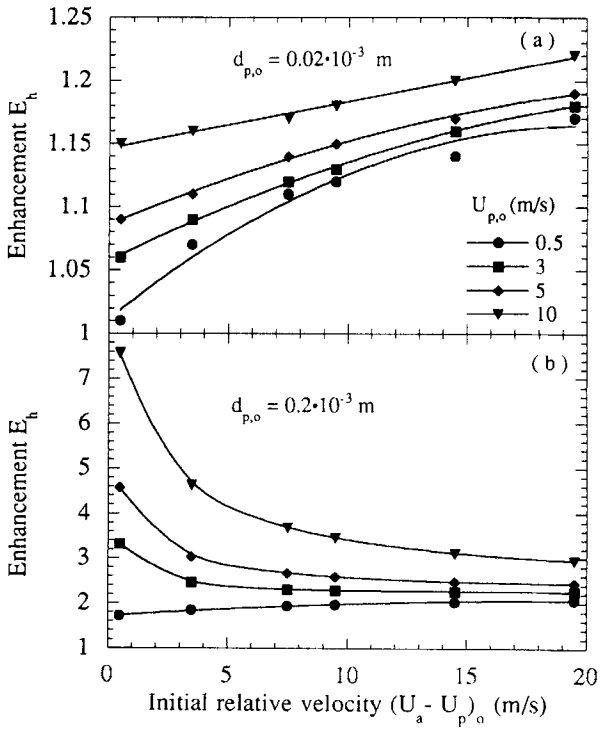

Figure 7. Effect of the initial droplet velocity $U_{p,o}$ on the enhancement.

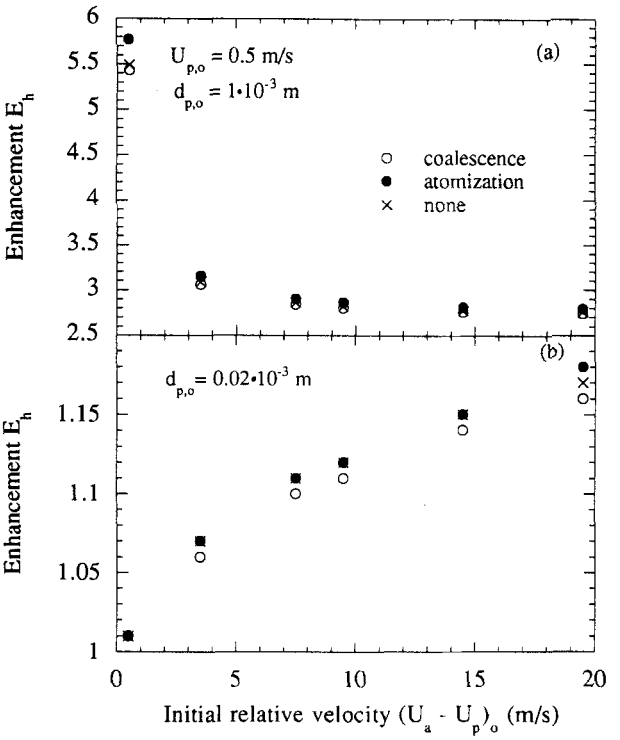

Figure 8. Effect of the atomization and coalescence on the enhancement.

Effect of atomization and coalescence on the enhancement

Additional effects investigated theoretically were atomization or coalescence of the droplets. The effect of atomization or coalescence on E_h was found generally negligible up to a $d_{p,o}$ of about 0.004 m, although atomization increased E_h and coalescence decreased it by comparison to conditions where these effects were absent. The effect was approximately 5%. The reason for this behavior is that atomization increases the surface area for heat transfer, on the one hand, but decreases the time the droplet remains in the system. The net effect therefore might not be significant, as shown in Figure 8. In addition, it was found that the effect of air temperature on E_h was negligible, in the range of 50 to 100°C.

A final remark on the agreement between the model predictions and the experimental results. In the experiments, $U_{p,o}$ and $d_{p,o}$ were not measured, but they can be estimated, that is, $d_{p,o}$ varies from 30 to 100 μm and $U_{p,o}$ is about 0.5 m/s. In agreement with these quantities, where $(U_a - U_p)_o \cong U_a$, Figure 6b shows the predicted behaviors of the enhancement E_h, which is similar to the one observed in Figure 4c. Thus, the model is partially confirmed.

Correlation of Data

It was assumed that the following independent variables influence h_v in evaporative cooling of gases:

$$h_v = f(k'_a, C_{p,a}, \rho_a, \mu_a, d, L, V_r, U_a). \tag{18}$$

The preceding equation was transformed into the following dimensionless expression by applying the Buckingham pi method.

$$\frac{d^2 h_v}{k'_a} = A\left(\frac{L}{d}\right)^{\alpha}\left(\frac{V_r}{L^3}\right)^{\beta}\left(\frac{U_a d}{\nu_a}\right)^{\gamma}\left(\frac{C_{p,a}\,\mu_a}{k'_a}\right)^{\delta}, \tag{19}$$

or alternatively

$$Nu = A\left(\frac{L}{d}\right)^{\alpha}\left(\frac{V_r}{L^3}\right)^{\beta} Re^{\gamma} Pr^{\delta} \tag{20}$$

where A and the exponents α to δ are adjustable parameters obtained by fitting the experimental data to the correlation. The following correlations were obtained by fitting the data for cylindrical coolers tested in evaporative cooling of air by

$$h_v = 3.31\times10^{-2} L^{-2.3}\left(\frac{V_r}{L^3}\right)^{-0.8} U_a^{1.7} \tag{21}$$

in units of h_v (W/m^3·K), L(m), V_r(m^3), U_a (m/s), where r = 0.961. In a dimensionless form it was obtained that

$$Nu = 1.96\times10^{-4}\left(\frac{L}{d}\right)^{-2.4}\left(\frac{V_r}{L^3}\right)^{-0.82} Re^{1.5}, \tag{22}$$

where r = 0.963. It is interesting to note that Eqs. 21 and 22 can be expressed with negligible error as

$$h_v = 3.31\times10^{-2} V_r^{-0.8} U_a^{1.7} \tag{23}$$

$$Nu = 11.96\times10^{4} V_r^{-0.8} Re^{1.5}. \tag{24}$$

Thus, only the volume of the reactor practically influences the heat-transfer process.

Various power input parameters were correlated as:

$$P'_l = 4.41\times10^{-6} L\left(\frac{V_r}{L^3}\right)^{0.12} U_a^{4.4} \tag{25}$$

where $P'_l(J/s) = Q_g \Delta P$ is the power input for transferring the air through the cooler where r = 0.931. It should be noted that the power input for atomizing water was negligible by comparison to the magnitude just given. In addition,

$$P_l = 4.4\times10^{-6} L^{-2}\left(\frac{V_r}{L^3}\right)^{-0.9} U_a^{4.4} \tag{26}$$

where P_l [(W)/m^3 reactor)] is a specific power with r = 0.960. Finally,

$$P_l = 54 L^{0.6} U_a^{2.4} \tag{27}$$

where P_l [(J/s)/(kg water evaporated)] is another specific power input with r = 0.780.

Calculations of a Cooling Cell

Usually, the initial and final temperatures of the gas (T_i, T_o) as well as its initial humidity (H_i) and flow rate (W_a) are given.

Thus, the final humidity of the gas is calculated from the following mass balance:

$$H_o = H_i + \frac{C_{p,a}}{\lambda}(T_i - T_o). \tag{28}$$

The final wet-bulb temperature of gas $T_{o,wb}$ is determined from T_o and H_o.

The quantity of water needed for cooling the gas is calculated from the heat balance

$$Q_w = \frac{C_{p,a}(T_i - T_o)}{\lambda} W_a. \tag{29}$$

Now, we choose the velocity of the gas at the inlet pipes, U_a, and determine their diameter from

$$d = \sqrt{\frac{2W_a}{\pi U_a \rho_a}}. \tag{30}$$

According to Eqs. 1 and 23 we can write

$$\frac{2.1\times10^{-2}}{d^2\rho_a} V_r^{0.2} U_a^{0.7} = \frac{(H_o - H_i)\lambda}{\Delta T_{lm}}, \tag{31}$$

which yields the volume of the cooling cell V_r, and ΔT_{lm} is determined from Eq. 2.

Finally, the diameter and length of the cooling cell are determined from the condition $5.5 \le L/d \le 13.3$.

Concluding Remarks

An evaluation of the performance of the evaporative cooler is based on a comparison of the volumetric heat-transfer coefficients. It should be noted that a direct comparison with a similar device is possible only with the work of Kondratov et al. (1989). Bearing in mind that the evaporation process is carried out in the constant rate evaporation regime, other comparisons are made with data of impinging-stream dryers. The comparison is shown in Table 2.

As seen, the maximum values of h_v for the evaporative cooler are lower than the values of impinging-stream dryers, but higher than the data for other devices. However, no data for the power input were found that could be used to evaluate the evaporative cooling device with others.

One should expect that by increasing the initial relative velocity between the phases that the enhancement E_h will always increase. However, as seen earlier, this behavior also depends on the size of the droplet. For example, if the diameter of the droplet is about 2×10^{-5} m, the enhancement will increase vs. $(U_a - U_p)_o$. On the other hand, if $d_{p,o} > 2\times10^{-4}$ m, the opposite behavior is expected. In our experiments, E_h always increased, indicating that the droplets' size was very small.

Table 2. Comparison of Volumetric Heat-Transfer Coefficients

Device	h_v(W/m^3·s)
Impinging-stream dryers (Tamir, 1994)	140 to 140,000
Other dryers (Tamir, 1994)	18 to 6,500
Evaporative cooler (Kondratov et al., 1989)	2,800 to 4,100*
This work	500 to 14,000

*h_v is not based on ΔT_{lm}, which is not reported.

Acknowledgment

Bin Yao gratefully acknowledges the scholarship provided by the Department of Chemical Engineering at Ben-Gurion University of the Negev.

Notation

$C_{p,a}$ = specific heat of air, J/(kg·K)
h = heat-transfer coefficient between the air and the droplet, W/(m^2·K)
k'_a = heat conductivity of air, W/(m·K)
L = length of cooler, m
P_l = specific power input—power needed to transfer the air through the cooler per its unit volumetric flow rate, (J/s)(m^3/s)
Pr = Prandtl number $C_{p,a}\,\mu_a/k'_a$, dimensionless
q = heat transfer rate, W
Q_g = volumetric flow rates of the air, m^3/s
Q_w = volumetric flow rate of water, m^3/s
r = correlation coefficient with maximal value of unity, dimensionless
$Re = Q_g\,\rho_a/(d\,\mu_a)$, dimensionless
$Re_p = d_p\,\rho_a/|U_a - U_p|/\mu_a$
T_l = water temperature at inlet of the cooler, K
U_a = uniform air velocity along the flow field, m/s
U_p = droplet velocity, m/s
t = time, s
λ = latent heat of vaporization, J/kg
μ_a = air viscosity, Ns/m^2
ρ_a = density of air, kg/m^3

Literature Cited

Bar, T., and A. Tamir, "An Impinging-Stream Reactor with Two Pairs of Tangential Air Feed," *Can. J. Chem. Eng.*, **68**, 541 (1990).

Bird, B., W. E. Stewart, and E. N. Lightfoot, *Transport Phenomena*, Wiley, New York (1960).

Champion, M., and P. A. Libby, "Reynolds Stress Description of Opposed and Impinging Turbulent Jets. Part I: Closely Spaced Opposed Jets," *Phys. Fluids*, **A 5**(1), 203 (1993).

Elperin, I., *Transport Processes in Impinging Jets*, in Russian, Nauka, Minsk, (1972).

Herbet, S., "Extraction in Impinging Streams," MSc Thesis, in Hebrew, Dept. of Chemical Engineering, Ben-Gurion University of the Negev, Beer-Sheva, Israel, in progress (1995).

Herskowits, D., V. Herskowits, and A. Tamir, "Desorption of Acetone in a Two Impinging Streams Spray Desorber," *Chem. Eng. Sci.*, **42**, 2331 (1987).

Herskowits, D., V. Herskowits, K. Stephan, and A. Tamir, "Characterization of a Two Phase Impinging Jets Absorber: I. Physical Absorption of Carbon Dioxide in Water," *Chem. Eng. Sci.*, **43**, 2773 (1988).

Kitron, A., R. Buchman, K. Luzzatto, and A. Tamir, "Drying and Mixing of Solids and Particles' RTD in Four Impinging Streams and Multistage Two Impinging Stream Reactors," *Ind. Eng. Chem. Res.*, **26**, 2454 (1987).

Kondratov, V. V., V. L. Meltzer, and A. Yu. Valberg, "Evaporative Cooling of Gases in an Apparatus with Counter Streams," in Russian, *Ind. Sani. Clean. Gases*, No. 2, 11 (1989).

Kostiuk, L. W., and P. A. Libby, "Comparison Between Theory and Experiment for Turbulence in Opposed Streams," *Phys. Fluids*, **A5**, 2301 (1993).

Kostiuk, L. W., K. N. C. Bray, and R. K. Cheng, "Experimental Study of Premixed Turbulent Combustion in Opposed Streams: I. Nonreacting Flow Field," *Comb. Flame*, **93**, 377 (1993).

Luzzatto, K. and A. Tamir, "Combustion of Gas in a Two Impinging Wall Jets Combustor," *Combustion Sci. Technol.*, **65**, 67 (1989).

Tamir, A., *Impinging-Stream Reactors—Fundamentals and Applications*, Elsevier, Amsterdam, p. 761 (1994).
Tamir, A., and I. Elperin, "Method, Device and Apparatus for Carrying Out Gas-Liquid Mass Exchange Operations and Process Employing the Same," Israeli Patent No. 73301 (Dec. 17, 1987).
Tamir, A., and A. Glitzenstein, "Modeling and Application of a Semibatch Coaxial Two-Impinging-Streams Contactor for Dissolution of Solids," *Can. J. Chem. Eng.*, **70**, 104 (1992).
Tamir, A., "Absorption of Acetone in a Two Impinging Streams Absorber," *Chem. Eng. Sci.*, **41**, 3023 (1986).
Tamir, A., and D. Herskowits, "Absorption of CO_2 in a New Two Impinging Streams Absorber," *Chem. Eng. Sci.*, **40**, 2149 (1985).
Tamir, A., and K. Luzzatto, "Solid-Solid and Gas-Gas Mixing Properties of a New Two Impinging-Stream Mixer," *AIChE J.*, **31**, 781 (1985a).
Tamir, A., and K. Luzzatto, "Mixing of Solids in Impinging Streams Reactors," *Powder Bulk Solids Technol.*, **9**, 15 (1985b).
Tamir, A., and S. Sobhi, "A New Two-Impinging-Streams Emulsifier," *AIChE J.*, **31**, 2089 (1985).
Tamir, A., I. Elperin, and K. Luzzatto, "Drying in a Two Impinging Streams Reactor," *Chem. Eng. Sci.*, **39**, 139 (1984).
Yao, B., "Evaporative Cooling of Air in Impinging Streams," MSc Thesis, Dept. of Chemical Engineering, Ben-Gurion University of the Negev, Beer-Sheva, Israel (1994).
Ziv, A., and A. Tamir, "Calcination of Phosphate in Impinging Streams: I. Development, Theory and Modeling," and A. Tamir, A. Ziv, E. Zeigerson, B. Parpar, E. Tovim, S. Sason, L. Zevin, and Y. Friedman, "Calcination of Phosphate in Impinging Streams: II. Phosphate with High Organic Matter and with Pulverized Coal," *Can. J. Chem. Eng.*, **71**, 771 (1993).
Ziv, A., K. Luzzatto, and A. Tamir, "Applications of Free Impinging Streams to the Combustion of Gas and Pulverized Coal," *Combustion Sci. Technol.*, **60**, 31 (1988).

Manuscript received Mar. 7, 1994, and revision received Sept. 6, 1994.